Experimental setup of a cascaded two-stage organic Rankine cycle

Frithjof H. Dubberke,[1] Matthias Linnemann,[1] Wameedh Khider Abbas,[1] Elmar Baumhögger,[1] Klaus-Peter Priebe,[1] Maximilian Roedder,[2] Matthias Neef,[2] and Jadran Vrabec[1, a)]

[1)] *Thermodynamik und Energietechnik, Universität Paderborn, Warburger Straße 100, 33098 Paderborn, Germany*

[2)] *Zentrum für innovative Energiesysteme, Hochschule Düsseldorf, Münsterstraße 156, 40476 Düsseldorf, Germany*

(Dated: 24 October 2017)

In combination with a bottoming cycle, operated with a pure fluid in transcritical mode, the usage of a zeotropic mixture as working fluids appears to be exergetically favorable for power cycle efficiency in cascaded two-stage organic Rankine cycles (CORC). A CORC is set up and initially tested with cyclopentane and propane as working fluids in its high temperature and low temperature cycle, respectively. A thermal oil cycle serves as the heat source and is powered electrically with a maximum heat flow of 158 kW. The design of this experimental setup allows for a rapid replacement of individual components and for a wide range of conditions in terms of fluids and thermodynamic states. The components of all cycles and the measurement and control technology are described in detail. A testing procedure is presented, followed by a discussion of the measurement results, where it is shown that the intended concept of two cascaded organic Rankine cycles is operational and that the measured data are consistent.

Keywords: organic Rankine cycle; cascade; multicomponent working fluid; temperature-glide; pinch point, exergetic efficiency

I. INTRODUCTION

Many types of organic Rankine cycles (ORC) for the recovery of waste heat have been described in the literature[1–5]. Different cycle layouts and components, combined with a variety of organic working fluids, lead to a wide range of power cycle efficiency values mainly due to the characteristics of the heat source. Lampe et al.[6] proposed a design tool to maximize process performance by optimizing both process parameters and varying the working fluid. Taking the economic situation of an individual project into account, cycle construction can be realized in a sophisticated way to reach higher power efficiency[7].

To maximize performance of ORC processes, the usage of mixtures as working fluids appears to be beneficial due to an exergetically favorable heat transfer caused by the temperature glide during evaporation[8,9]. Having a more constant temperature difference ΔT while transferring heat from the heat source due to the temperature glide of zeotropic mixtures may minimize exergetic losses[10]. On the other hand, the temperature glide is exergetically unfavorable during condensation and may neutralize the exergetic advantage during evaporation. Therefore, a second low temperature (LT) cycle was coupled in this work as a cascade to utilize the residual exergy that is discharged by the condenser of the high temperature (HT) cycle[11–13]. Thus, a cascaded two-staged ORC, where the HT cycle is operated with a zeotropic mixture and the LT cycle is operated with a pure fluid in transcritical mode[14], may facilitate both heat uptake from the source as well as heat discharge to the environment in a favorable way.

As a test rig for two-stage cycle innovations, an electrically heated cascaded ORC (CORC) was designed and commissioned in Paderborn. To achieve a high efficiency, the design strongly depends on the temperature level of the heat source. The integration of four electrical heating rods as a primary heat source for the HT cycle enabled for the specification of different temperature levels and the LT cycle was supplied with the residual thermal energy discharged by the HT cycle. After successful commissioning of the two-stage CORC, experimental results were used to evaluate component and cycle performance in comparison to the intended design. Fig. 1 (left) shows the non-isothermal heat flow $\dot{Q}$, formally separated into the exergy flow $\dot{E}$ and anergy flow $\dot{A}$, which is determined by the ambient temperature T_a in a temperature-entropy diagram[15]. For a non-isothermal heat source, $\dot{E}$ ranges from the inlet temperature T_{in} down to T_a. Fig. 1 (right) illustrates a combination of two pure fluids that exemplify heat integration between the HT and LT cycles and their exergetic utilization of a given heat source. State points 2 to 3 outline the exergy uptake of the HT cycle and state points B to C outline the exergy uptake of the LT cycle. The pinch point characterizes the minimum temperature difference ΔT^{pp} during the heat transfer to the HT and LT cycle.

A feature of the present CORC test rig is that individ-

[a)] corresponding author, tel.: +49-5251/60-2421, fax: +49-5251/60-3522, email: jadran.vrabec@upb.de

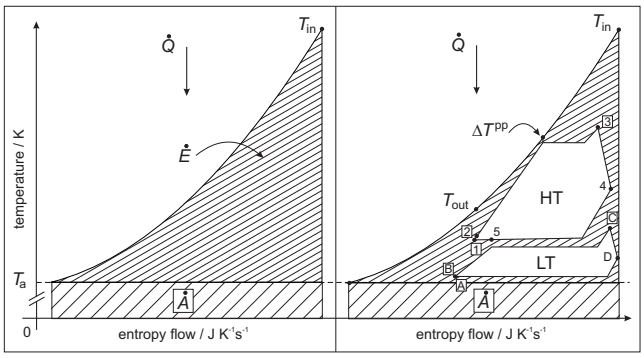

FIG. 1. (left) Exergy flow ($\dot{E}$) and anergy flow ($\dot{A}$) of a non-isothermal heat source for ambient temperature T_a. (right) Potential arrangement of high temperature (HT) and low temperature (LT) cycles of the CORC to maximize the utilization of the exergy flow $\dot{E}$, cf. Baehr[16].

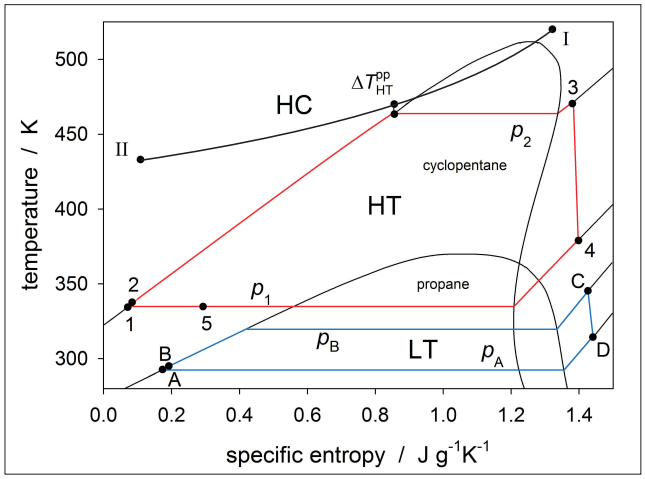

FIG. 2. CORC process in a temperature-entropy diagram: the high temperature (HT) cycle operated with cyclopentane was driven by the heating cycle (HC); the low temperature (LT) cycle operated with propane and was connected to the HT cycle by a heat exchanger acting as a condenser for the HT cycle and an evaporator for the LT cycle. The pinch point characterizes the minimum temperature difference $\Delta T_{\mathrm{HT}}^{\mathrm{pp}}$ between the HC and the HT cycle during heat transfer, cf. DiPippo[9].

ual components, such as heat exchangers, pumps, condensers, turbines as well as working fluids, can be varied rapidly at comparably low cost. The long-term goal of the present project is to put a two-stage CORC system into practice, exploiting waste heat sources at temperature levels above 600 K, particularly from biogas engines. An additional target is to identify combinations of working fluids (pure fluids and mixtures) that may exploit a maximum of the incoming exergy from waste heat sources, cf. Fig 1 (right).

Instead of a zeotropic mixture, cyclopentane was chosen in this work as the working fluid for the HT cycle for testing reasons, following a recommendation by Lai et al.[17], and propane was chosen as the working fluid for the LT cycle. Propane was proposed by Schilling et al.[18] for low temperature applications. With a critical temperature of $T_c = 369.8$ K it is suitable for transcritical operation at a comparably low temperature. Fig. 2 shows potential thermodynamic state points in a temperature-entropy diagram for the present working fluid selection of the CORC, where the HT cycle was operated with cyclopentane and the LT cycle with propane.

The use of an internal heat exchanger (IHE) was not considered in this work because it does not affect the exergetic efficiency. It impacts the thermal efficiency which is governed by the temperature level of the heat transfer and is not suitable for rating the performance of a cycle exploiting a non-isothermal heat source[19].

II. CORC APPARATUS SETUP

Due to safety reasons, e.g. because flammable working fluids may be employed, the CORC was placed outside of the laboratory in a separate container. Both the HT and LT cycle were designed according to AD 2000-Regelwerk B7 (HT / LT in PN 100 / PN 60). All flanges were sealed with meshed metal (chrome-nickel-molybdenum alloy, Material-Nr. 1.4404) strengthened graphite gaskets novaphit SSTCTA-L provided by Frenzelit[20], limiting the leakage rate to a tolerable amount which was assessed by pressure tests.

To ensure that the maximum working temperature of 353 K of the pressure sensors (6.4 MPa) was not exceeded, a flexible metal tube was used as an extension which was connected with a tube fitting to the piping system and sealed with a copper gasket and PTFE sealing.

A. Heating cycle

The heating cycle (HC) mass flow was driven by a pump (Allweiler NTWH 25 200/01; 0.3 kW), which was capable of a feeding mass flow of up to 700 g/s of Therminol 66[21]. Heat was supplied by four electrical heating rods with a combined power of 158 kW, three with 50 kW and one with 8 kW. One 50 kW heating rod was thyristor-controlled (TCH) and fully adjustable, the three remaining ones were controlled by power contactors (PCH). Consequently, the combination of all four heating rods enabled for a variable heating power from 0 to 158 kW, where switching of the PCH was necessary. Fig. 5 (top) illustrates the heating concept by depicting total power, which results from the sum of the TCH and the three PCH, over increasing or decreasing heating power. The switching points were chosen differently, depending on increasing or decreasing heating power, which led to a switching offset of 8 kW. This strategy supported a more

FIG. 3. CORC setup in a container that was placed outside of the laboratory due to safety reasons. Heat exchangers and piping system were thermally insulated with mineral wool.

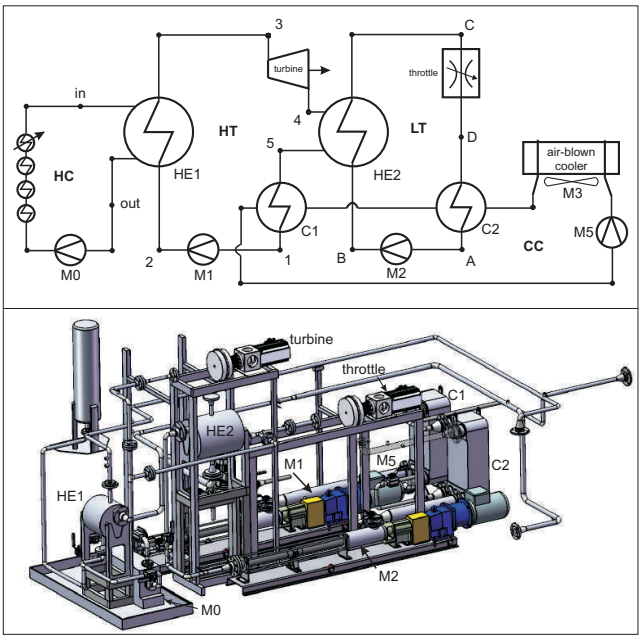

FIG. 4. (top) Design of the experimental CORC setup: a high temperature (HT) and a low temperature (LT) cycle were coupled to a cascade (CORC) by a heat exchanger (HE2) to maximize exergetic utilization. The heating cycle (HC) was realized by four electrical heating rods and a pump (M0). Heat was discharged from the HT and LT cycles to the ambient by an air-blown cooler (M3) using a ethylene-glycol/water mixture, which was pumped (M5) through the cooling cycle (CC) via condensers (C1, C2) in the HT and LT cycle. (bottom) CORC construction layout: HT heat exchanger (HE1) and feed pumps (M1, M2) of the HT and LT cycles, respectively. For the present testing reasons, the LT cycle had a variable throttle as an expansion device instead of a turbine.

rapid attainment of stationary operation, in particular a stable inlet temperature T_{in} at the evaporator.

B. High and low temperature cycles

The main difference between the two cycles was that the HT cycle had a turbine, while a variable throttle was used as an expansion device in the LT cycle. This was done for practical reasons, since at this stage of the experiment the thermodynamic conditions, which are essential for the design of a turbine, were not constrained for the LT. The HT cycle was filled with about 40 kg of cyclopentane and the LT cycle with about 20 kg of propane. Both cycles were pressure tested up to a pressure of 4 MPa (HT) or 6 MPa (LT).

C. Feed pumps

Progressive cavity pumps (NETZSCH NEMO®[22]) were applied as feed pumps (M1, M2), which worked with a helical rotor inside a helical stator. This type of pump is capable to deal with two-phase fluids, is not susceptible to cavitation and works up to high pressures. The emerging cavities between rotor and stator move along the axis and transport the fluid. These cavities do not change in their size and are sealed among each others so that volume flow is controlled by rotational speed. Disadvantages of this type of pump are that they may not run dry and that the pumped fluid must be harmonized with the material of the stator. Typically, this material selection is preceded by chemical compatibility and moisture expansion tests.[23] Modification of the stator geometry, such as expansion due to temperature or chemical non-compatibility, may lead to a decrease of pump efficiency or even to failure. For pumping propane in the LT cycle, glycerin was used as a friction modifier, as described by Hadfield et al.[24] and Granryd[25]. Approximately 100 g of glycerin was placed directly in the inlet of the stator on the suction side.

D. Heat exchanger

Plate and shell heat exchangers from Vahterus[26] were applied as HE1 and HE2 with a total volume of 13 l and 25 l. Their operation pressure range of up to 6 MPa for HE1 and up to 10 MPa for HE2 was large. In combination with the maximum design temperature of 523 K, they allow for the study of a wide range of thermodynamic states. In both cases, evaporation of the working fluids took place in the plate of the heat exchanger due to higher flow velocity of the steam which led to a higher heat transfer coefficient. To ensure a proper steam qual-

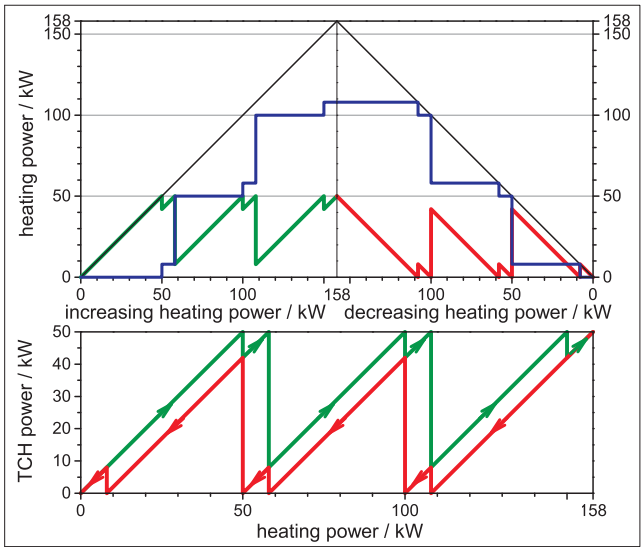

FIG. 5. (top) Heating concept: combination of three power contactors heating rods (PHC, blue) and one thyristor controlled heating rod (THC) with a different switching strategy for increasing (green) and decreasing (red) total heating power output (black) to avoid excessive switching due to a small hysteresis. (bottom) THC power over total heating power in case of increasing (green) or decreasing (red) total heating power output.

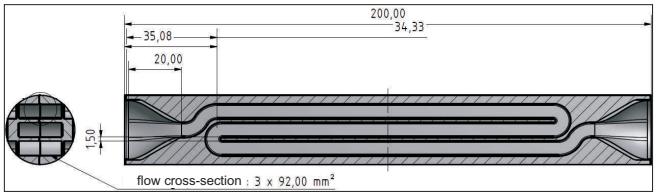

FIG. 6. Cut through the demister, which reversed the flow direction of the steam twice within a tube geometry. At high flow velocities, liquid droplets, which may be carried by the superheated steam, centrifuge to the outer edges of the tube and evaporate. All lengths are given in millimeter.

ity, a demister was connected downstream to HE1 in the HT cycle. It reversed the flow direction of the steam twice within a tube geometry. At high flow velocities (here about 13 m/s) liquid droplets, which may be carried by the superheated steam, centrifuge to the outer edges of the tube and evaporate at the tube surface, cf. Fig. 6.

E. Cooling cycle

The overall waste heat was discharged via an air-blown cooler (type H.T.E.) outside of the container by a cooling cycle, which was connected to the condensers C1 and C2 (plate heat exchangers type GEA WTT PL 150) of the HT and LT cycles. It operated on the basis of a binary ethylene-glycol/water (1 : 1.125) mixture driven by pump M5 (Grundfos TP 50-120/2) with a volume flow of about 17.6 m^3/h. M5 circulated the cooling liquid through C1 and C2, where residual heat was taken after the turbine from the HT cycle and after the throttle from the LT cycle, cf. Fig. 4 (top).

F. Turbine and generator

The design of the CORC turbine was based on an axially fed centrifugal pump that expanded the superheated vapor through its curved laval nozzles that were embedded in a blade wheel (1.4305 / X8CrNiS) outwards to the radial expansion tube in the turbine casing (1.4006+QT / X12Cr13), cf. Fig. 7. Due to the impulse principle, the torque was mainly generated by the acceleration of the high velocity flow in the blades, as described e.g. by Fister[27]. The connection between turbine and generator, which was a six pole synchronous servomotor operating at 50 Hz (type SK-190-1-30-560 T1), was maintained by non-contacting magnetic coupling. The synchronous machine switches from motor to generator operation, as soon as the force of the steam exceeds the break loose torque of the driving shaft. To minimize gap losses in the CORC turbine, the gap was designed as a labyrinth seal with 12 steps with a width of 0.25 mm and a rotary shaft seal. Two angular ball bearings in O arrangement and one deep groove ball bearing formed the fixed shaft bearing at the turbine side, which lead to a minimum slackness of the blade wheel. For cooling and lubrication of the ball bearings, the casing was flodded with hydraulic oil (Mobil DTE 10 EXCEL 15). The construction of the wheel blade enabled for a quick and easy adaption to different thermodynamic states for varying working fluids at low cost. The focus of this turbine lied on its applicability for testing a large variety of working fluids over a wide range of thermodynamic states and therefore the efficiency was subordinate at this point in time. A variable throttle in the LT cycle allowed adjusting a suitable expansion ratio, according to mass flow and fluid properties.

G. Controller and sensors

The CORC software framework was based on two systems: a graphical user interface (GUI), which was programmed in Agilent VEE, and a C program providing functions for the GUI to access the programmable logic controller (PLC). The PLC allowed for digital in- and output (DI/DO) and analog in- and output (AI/AO), which expect either a voltage from 0 to 10 V, a current from 4 to 20 mA or a resistance from temperature (Pt1000) and pressure sensors. The AO connectors were used for setting the motor speed of the pumps by sending a signal from 0 to 10 V to these devices. The DI could only detect an activated (24 V) or deactivated voltage (0 V) and was used for receiving error status from the devices. With the DO, variable-frequency drivers (VFD) or

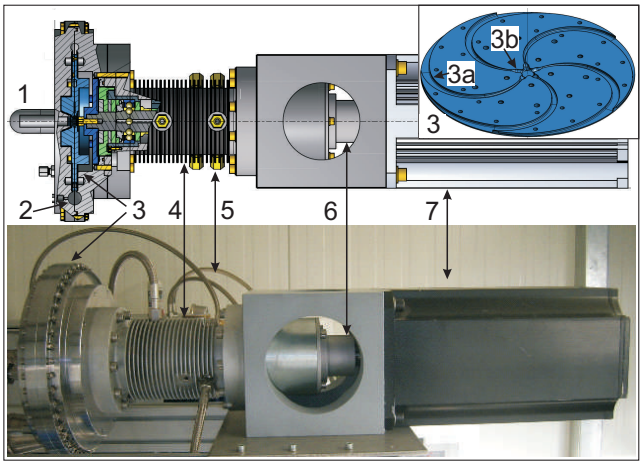

FIG. 7. Centrifugal radial turbine with two angular ball bearings and a magnetic coupling to the generator: (1) axial steam inlet; (2) steam outlet; (3) blade wheel; (3a) blade channel; (3b) laval nozzle; (4) shaft bearing; (5) cooling and lubrication cycle; (6) magnetic coupling; (7) generator.

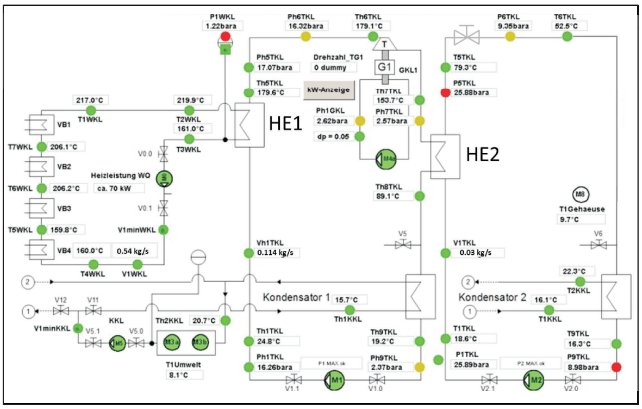

FIG. 8. CORC master display visualizing the hydraulic schematic with the essential operation parameters, such as temperatures and pressures of the HC, the HT and LT cycles as well as the CC. It enabled for an operation of the actors and allowed to set different thermodynamic states within the cycles.

non-controllable actors were turned on and off by sending a current to them or their dedicated contactors. All in- and output streams were monitored and accessed by the GUI. An alternative to the PLC was a hard-wired programmed logic controller (HPC), which was used for safety functions. A VFD, that is often applied in electromechanical systems as a frequency converter, was used to control the pumps and the generator. The mass flow measurement in the HT and LT cycles worked with a differential pressure aperture according to DIN EN ISO 5167.

H. Safety precautions

Working with the CORC mandated dedicated safety requirements because flammable and potentially hazardous fluids were employed at high temperatures and pressures. The experimental setup was therefore placed in a container outside of the laboratory. A gas leakage monitoring system with an infrared gas transmitter sensor (Dräger Polytron IR type 334)[28] calibrated for hydrocarbons was linked to an electric autonomous ventilation system as explosion prevention to avoid a flammable atmosphere in the container. In addition, any gas detection would have triggered an emergency shutdown and switched all electric parts to dead voltage, preventing igniting sparks. Redundant temperature and pressure sensors were hard-wired programmed for the feed pumps M1 to a maximum pressure of 3.5 MPa and M2 to a maximum pressure of 2.5 MPa as well as to the HC to a maximum temperature of 573 K. A manual emergency valve was implemented in the LT cycle for releasing its working fluid (here propane) outside of the container.

III. EXPERIMENTAL SETUP AND INITIAL OPERATION

The initial operation aimed at the evaluation of the components of the experimental setup and the basic function of the apparatus, namely exploiting a heat source by two cascaded cycles. At this stage, the focus lied on the heat exchangers, especially HE2 coupling the two cycles as the central element of the cascade. Before start up, a variety of technical preparations was required. Before and during the filling of the HT cycle with cyclopentane, inert gas was removed by a vacuum pump in combination with a cooling trap. The LT cycle was evacuated before its filling. To enhance the filling process the pressure difference between the propane gas bottle and the LT cycle was increased. Therefore, the temperature of the propane gas bottle, which was hung upside down to force the liquid phase into the hose, was raised by about 15 K above ambient temperature. Because of the flammability of cyclopentane and propane, as a mandatory safety procedure, the ventilation system of the container (open doors) was activated and access to the laboratory was prohibited. The positioning of all valves was checked. First, the heating cycle was warmed up along a temperature ramp and the cooling cycle was activated at the same time. Before the mass flow of M1 in the HT cycle was gradually increased and the turbine was set to 50 Hz rotation, lubrication and the cooling cycle of the turbine ball bearing started. Subsequently, the mass flow of the HT cycle $\dot{m}_{\mathrm{HT}}$ was raised by feed pump M1 until a heat flow of about $\dot{Q}_{\mathrm{HT}} = 70$ kW was transferred from the HC to the HT cycle at constant quality of evaporation (dry steam) behind the demister.

IV. PERFORMANCE OF HEAT TRANSFER

Because the CORC was based on two cascaded cycles, HE2 played a major role as the central element transferring heat from the HT cycle to the LT cycle. The dimensioning and layout design of HE2 determined the overall cycle performance. Therefore, at this stage of the experimental setup it was important to learn about the characteristics of HE 2 due to its process parameters, such as mass flow and temperature, as a function of the thermophysical properties of the working fluids. To simplify this complex interrelationship, the inlet temperature T_{in} of the HC was controlled at 493 K for a constant mass flow of about 0.5 kg/s of Therminol 66®, whereas the mass flows of the working fluids driven by the feed pumps M1 and M2 were variable parameters. All subordinate parameters were derived from this setting. This knowledge enables for an optimization of future cycle design and operation. For a proper validation of all heat exchangers, the balancing calculations were done on the basis of a steady state flow process.

A constant heat flow $\dot{Q}_{\mathrm{HC}} = 70$ kW from the HC led to an enthalpy flow $\Delta\dot{H}$ into the HT cycle, where isobaric conditions were assumed in the heat exchanger. Feed pump M1 pressurized a mass flow of about $\dot{m}_{\mathrm{HT}} = 0.110$ kg/s of cyclopentane to a pressure of 1.6 MPa. It was preheated from state point 2 at a temperature of $T_2 = 297$ K and an enthalpy of $h_2 =$ -46.32 kJ/kg, evaporated and superheated to a temperature of $T_3 = 452$ K at state point 3. In addition to the measured temperature and pressure data, other thermodynamic properties were derived with REFPROP[29], based on accurate equations of state (EOS) from Gedanitz et al.[30] for cyclopentane and from Lemmon et al.[31] for propane.

The pinch point temperature difference $\Delta T_{\mathrm{HT}}^{\mathrm{pp}}$ between the HC and HT cycle in HE1 was determined by equating the heat flow from state points 2 to s_{HT} (saturated liquid) in the HT cycle and state points II to pp of the HC

$$-\dot{Q}_{\mathrm{II,pp}} = \dot{Q}_{2,s_{\mathrm{HT}}}. \tag{1}$$

The heat flow in this section of the HT cycle was

$$\begin{aligned}\dot{Q}_{2,s_{\mathrm{HT}}} &= \dot{m}_{\mathrm{HT}} \cdot (h^s_{\mathrm{HT}} - h_2) \\ &= 0.11\ \frac{\mathrm{kg}}{\mathrm{s}} \cdot (273.67 - (-46.32))\ \frac{\mathrm{kJ}}{\mathrm{kg}} \\ &= 35.2\ \mathrm{kW},\end{aligned} \tag{2}$$

where the saturated liquid state point s_{HT} of the HT cycle with its temperature $T^s_{\mathrm{HT}}(1.6\ \mathrm{MPa}) = 441.15$ K and has an enthalpy $h^s_{\mathrm{HT}}(1.6\ \mathrm{MPa}) = 273.67$ kJ/kg. With an average isobaric heat capacity of $\bar{c}_{\mathrm{p}}^{\mathrm{T}} = 2.19$ kJ/kg K of Therminol, the heat flow in this section of the HC was

$$\dot{Q}_{\mathrm{II,pp}} = \dot{m}_{\mathrm{HC}} \cdot \bar{c}_{\mathrm{p}}^{\mathrm{T}} \cdot (T_{\mathrm{II}} - T_{\mathrm{HC}}^{\mathrm{pp}}). \tag{3}$$

With the knowledge of the pinch point temperature of the Therminol

$$\begin{aligned}T_{\mathrm{HC}}^{\mathrm{pp}} &= \frac{\dot{Q}_{\mathrm{II,pp}}}{\dot{m}_{\mathrm{HC}} \cdot \bar{c}_{\mathrm{p}}^{\mathrm{T}}} + T_{\mathrm{II}} \\ &= \frac{-35.2\ \mathrm{kW}}{0.54\ (\mathrm{kg\ s^{-1}}) \cdot 2.19\ (\mathrm{kJ\ kg^{-1}\ K^{-1}})} + 434.15\ \mathrm{K} \\ &= 463.91\ \mathrm{K},\end{aligned} \tag{4}$$

the pinch point temperature difference was given

$$\Delta T_{\mathrm{HT}}^{\mathrm{pp}} = T^s_{\mathrm{HT}} - T_{\mathrm{HC}}^{\mathrm{pp}} = (463.91 - 441.15)\ \mathrm{K} = 22.7\ \mathrm{K}. \tag{5}$$

In this work, the design of the turbine in the HT cycle was not optimized for cyclopentane. Therefore, a nearly isoenthalpic expansion in the radial turbine to a pressure

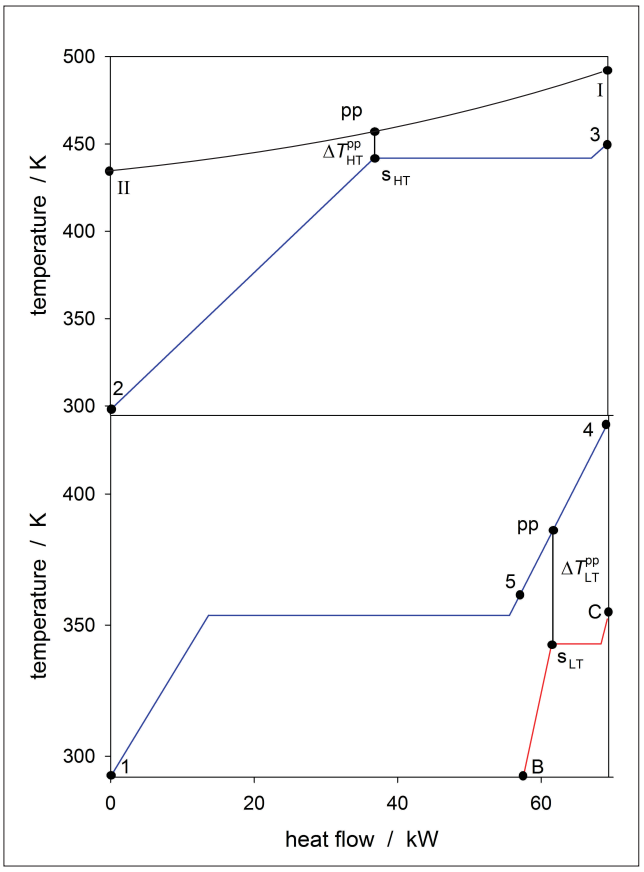

FIG. 9. (top) Heat transfer in HE1: Therminol 66® (black) from the HC supplied a heat flow of 70 kW to the HT cycle, where a mass flow of cyclopentane (red) was heated, evaporated and superheated from state point 2 to state point 3 at a pressure of $p_2 = 1.6$ MPa. (bottom) Heat transfer in HE2: the LT cycle absorbed a heat flow of 12.32 kW from the HT cycle (red) to heat, evaporate and superheat a mass flow of propane (blue) from state point B to state point C at a pressure of $p_{\mathrm{B}} = 2.56$ MPa. Residual heat from the HT and LT cycles was discharged via the condensers C1 and C2. The pinch point temperature difference in HE2 $\Delta T_{\mathrm{LT}}^{\mathrm{pp}} = 43.9$ K was about twice as large as the one in HE1 $\Delta T_{\mathrm{HT}}^{\mathrm{pp}} = 22.7$ K.

$p_1 = 0.23$ MPa led to an inlet temperature to the HE2 of $T_4 = 426.84$ K at state point 4. Between state points 4 and 5 cyclopentane was cooled in its gas state down to a temperature $T_5 = 362$ K.

The mass flow of propane in the LT cycle $\dot{m}_{\mathrm{LT}}$ was gradually raised by feed pump M2 until the temperature difference between inlet temperature T_4 and outlet temperature T_{C} of HE2 was reduced down to $\Delta T_{4,\mathrm{C}} = 74.4$ K. At the same time, the adjustable throttle was continuously controlled manually so that pressure p_2 reached about 2.58 MPa, which led to a mass flow of $\dot{m}_{\mathrm{LT}} = 0.03$ kg/s. Here, the heat flow

$$\begin{aligned}\dot{Q}_{\mathrm{B,C}} &= \dot{m}_{\mathrm{LT}} \cdot (h_{\mathrm{C}} - h_{\mathrm{B}}) \\ &= 0.03 \ \frac{\mathrm{kg}}{\mathrm{s}} \cdot (659.02 - 248.35) \ \frac{\mathrm{kJ}}{\mathrm{kg}} \\ &= 12.32 \ \mathrm{kW},\end{aligned} \tag{6}$$

was transferred via HE2 from the HT to the LT cycle. The pinch point temperature difference $\Delta T_{\mathrm{LT}}^{\mathrm{pp}}$ in the LT cycle was determined from the equality of the heat flows

$$-\dot{Q}_{\mathrm{pp},4} = \dot{Q}_{s_{\mathrm{LT}},\mathrm{C}}, \tag{7}$$

with

$$\begin{aligned}\dot{Q}_{s_{\mathrm{LT}},\mathrm{C}} &= \dot{m}_{\mathrm{LT}} \cdot (h_{\mathrm{C}} - h_{\mathrm{LT}}^{s}) \\ &= 0.03 \ \frac{\mathrm{kg}}{\mathrm{s}} \cdot (659.02 - 401.91) \ \frac{\mathrm{kJ}}{\mathrm{kg}} \\ &= 7.71 \ \mathrm{kW}.\end{aligned} \tag{8}$$

The saturated liquid state point s_{LT} of propane in the LT cycle had a temperature $T_{\mathrm{LT}}^{s}(2.58 \ \mathrm{MPa}) = 343.01$ K and enthalpy $h_{\mathrm{LT}}^{s}(2.58 \ \mathrm{MPa}) = 401.91$ kJ/kg. With the knowledge that heat was transferred only from superheated steam between state points 4 and 5 of the HT to the LT cycle, the heat flow was given by

$$\dot{Q}_{\mathrm{pp},4} = \dot{m}_{\mathrm{HT}} \cdot \bar{c}_{\mathrm{p}}^{\mathrm{c}} \cdot (T_4 - T_{\mathrm{LT}}^{\mathrm{pp}}). \tag{9}$$

Here, an average isobaric heat capacity of cyclopentane

$$\bar{c}_{\mathrm{p}}^{\mathrm{c}}(406.92 \ \mathrm{K}, 0.23 \ \mathrm{MPa}) = 1.758 \ \frac{\mathrm{kJ}}{\mathrm{kg} \cdot \mathrm{K}}, \tag{10}$$

was assumed. With the knowledge of the pinch point temperature derived from Eq. (9),

$$\begin{aligned}T_{\mathrm{HT}}^{\mathrm{pp}} &= \frac{\dot{Q}_{\mathrm{pp},4}}{\dot{m}_{\mathrm{HT}} \cdot \bar{c}_{\mathrm{p}}^{\mathrm{c}}} + T_{\mathrm{C}} \\ &= - \frac{-7.71 \ \mathrm{kW}}{0.11 \ (\mathrm{kg \ s^{-1}}) \cdot 1.758 \ (\mathrm{kJ \ kg^{-1} \ K^{-1}})} \\ &\quad + 426.8 \ \mathrm{K} \\ &= 386.96 \ \mathrm{K},\end{aligned} \tag{11}$$

the pinch point temperature difference was determined

$$\Delta T_{\mathrm{LT}}^{\mathrm{pp}} = T_{\mathrm{HT}}^{\mathrm{pp}} - T_{\mathrm{LT}}^{s} = (386.9 - 343) \ \mathrm{K} = 43.9 \ \mathrm{K}. \tag{12}$$

Since the turbine of the HT cycle did not yield any significant power output and a throttle was applied in the LT cycle, the overall heat of about 70 kW was dissipated by the air blown cooler to the ambient with the condensers C1 between the state points 5 and 1 in the HT cycle and with C2 between the state points D and A in the LT cycle. Because the dimensioning of C1, C2 and the air-blown cooler were excessively large, the dissipation of the waste heat from HT and LT cycles was done at a small temperature difference of $\Delta T < 8$ K.

V. CONCLUSION

The combination of zeotropic mixtures and pure working fluids in two-staged ORC applications may be exergetically favorable due to small temperature differences during heat exchange. The CORC process was constructed by coupling a HT and a LT cycle as a cascade that allows for different test modes. In the present experiment, the overall functionality and of all equipment parts was tested with the pure fluids cyclopentane and propane operating in the HT cycle and the LT cycle, respectively. The focus of the experiment was on the heat transfer between the two cycles. It was shown that the setup enables to partially use the waste heat from the HT to evaporate the LT working fluid. However, the majority of the waste heat from the HT, particularly most of the heat from condensation, was not transferred to the LT. In the future more suitable fluid pairs, including zeotropic mixtures, have to be identified that allow larger mass flows and with this a better thermal integration. To clarify the advantages of a two-staged ORC, the temperature of the heating cycle should be increased. Moreover, the design of the turbine in the HT cycle needs to be adapted to the thermodynamic state of its operation condition and the throttle needs to be replaced by a turbine in the LT cycle.

VI. ACKNOWLEGDEMENTS

The authors gratefully acknowledge fruitful discussions with Johann Fischer, Universität für Bodenkultur Wien, and Deutsche Forschungsgemeinschaft (DFG) for funding the experimental CORC setup.

[1] S. Lecomptea and H. Huisseune, Renew. Sustain. Energy Rev. **47**, 448 (2015).
[2] S. Amicabilea and J. Lee, Appl. Therm. Eng. **87**, 574 (2015).
[3] J. Song and C. Gu, Energy Convers. Manage. **105**, 995 (2015).
[4] A. Schuster, S. Karellas, and R. Aumann, Energy **35**, 1033 (2010).
[5] H. Chen, D. Y. Goswami, M. M. Rahman, and E. K. Stefanakos, Energy **36**, 549 (2011).
[6] M. Lampe, M. Stavrou, H. M. Bücker, J. Gross, and A. Bardow, Ind. Eng. Chem. Res. **53**, 8821 (2014).

TABLE I. Nomenclature

abbreviation	description	unit
AI / AO	analog input / output	[-]
C	cycle or condenser	[-]
CC	cooling cycle	[-]
CORC	cascaded two-stage organic Rankine cycle	[-]
DI / DO	digital input / output	[-]
EOS	equation of state	[-]
GUI	graphical user interface	[-]
HC	heating cycle	[-]
HT	high temperature cycle	[-]
LT	low temperature cycle	[-]
M	motor or feed pump	[-]
ORC	organic Rankine cycle	[-]
PCH	power contactor controlled heating rod	[-]
PLC	programmable logic controller	[-]
pp	pinch point	[-]
TCH	thyrister controlled heating rod	[-]
VFD	variable-frequency driver	[-]
h_i	specific enthalpy at state i	[J g^{-1}]
$\dot{m}$	mass flow	[g s^{-1}]
$\dot{Q}$	heat flow	[J s^{-1}]
s	specific entropy	[J g^{-1} K^{-1}]
S	entropy	[J K^{-1}]
T	temperature	[K]

[7] L. Tocci, T. Pal, I. Pesmazoglou, and B. Franchetti, Energies **10**, 1 (2017).
[8] G. Angelino and P. Colonna, Energy **23**, 449 (1998).
[9] R. DiPippo, Geothermics **33**, 565 (2004).
[10] N. Eğrican and S. Uygur, Energy Convers. Manage. **32**, 375 (1991).
[11] B. Liu, P. Rivière, C. Coquelet, R. Gicquel, and F. David, Appl. Energ. **100**, 285 (1985).
[12] G. Shu, L. Liu, H. Tian, H. Wei, and Y. Liang, Energy Convers. Manage. **76**, 234 (2013).
[13] M. Mehrpooya, M. Ashouri, and A. Mohammadi, Energy **126**, 899 (2017).
[14] Z. Shengjun, W. Huaixin, and G. Tao, Appl. Energ. **88**, 2740 (2011).
[15] Z. Rant, Forsch. Ing. Wes. **22**, 36 (1956).
[16] H. D. Baehr, *Thermodynamik: Eine Einführung in die Grundlagen und ihre technischen Anwendungen; mit 80 Beispielen*, 4th ed. (Springer, Berlin, 1978).
[17] N. A. Lai, M. Wendland, and J. Fischer, Energy **36**, 199 (2011).
[18] J. Schilling, M. Lampe, J. Gross, and A. Bardow, Chem. Eng. Sci. **159**, 217 (2017).
[19] M. Yari, Renew. Energ. **35**, 112 (2010).
[20] Frenzelit, *novaphit® SSTC Technical Datasheet* (Frenzelit Werke).
[21] FRAGOL, *Therminol 66® Produktinformation* (FRAGOL SCHMIERSTOFF).
[22] NETZSCH Pumpen und Systeme, *NEMO® Progressing Cavity Pumps* (NETZSCH Pumpen und Systeme, 2015).
[23] NETZSCH Incorporated, *NEMO-NM MINI: Operating and Maintenance Instruction* (NETZSCH NEMO® Pump, 1999).
[24] N. P. Garland and M. Hadfield, Mater. Design **26**, 578 (2005).
[25] E. Granryd, Int. J. Refrig. **24**, 15 (2001).
[26] VAHTERUS, *Plate & Shell® Heat Exchanger* (VAHTERUS, Finland, 2014).
[27] W. Fister, *Fluidenergiemaschinen* (Springer Verlag, Berlin, Heidelberg, 1984).
[28] Dräger Safety, *Dräger Polytron IR type 334 and type 340* (Dräger Safety, 8th edition, 2008).
[29] E. Lemmon, M. Huber, and M. McLinden, *Reference Fluid Thermodynamic and Transport Properties REFPROP, Version 9.1, 2013* (National Institute of Standards and Technology, Standard Reference Data Program, Gaithersburg, 2013, 2013).
[30] H. Gedanitz, M. J. Davila, and E. W. Lemmon, J. Chem. Eng. Data **60**, 1331 (2015).
[31] E. W. Lemmon, M. O. McLinden, and W. Wagner, J. Chem. Eng. Data **54**, 3141 (2009).